Angular distributions in photodetachment from O^-

D. Hanstorp and C. Bengtsson
Department of Physics, Chalmers University of Technology and University of Göteborg, S-412 96, Sweden

D. J. Larson
Department of Physics, University of Virginia, Charlottesville, Virginia 22901
(Received 9 March 1989)

The angular distributions of electrons photodetached from a beam of negative oxygen ions have been measured at photon energies ranging from 1.7 to 2.7 eV. The calculation of asymmetry parameters for negative ions is briefly discussed, and the parameters derived from the measurements are compared with calculations and other measurements.

I. INTRODUCTION

Angular distributions of photoelectrons have been studied in many experiments on atomic photoionization.[1] Unlike total cross sections, differential-cross-section measurements provide data not only on the magnitudes of the relevant transition amplitudes but also on their relative phases. The photoionization angular distributions generally undergo variations near threshold, near the Cooper minimum, and in the vicinity of resonances. Calculations show that the distributions are sensitive to ground-state correlations, interchannel coupling, anisotropic electron-ion interactions, and relativistic effects.[2,3] Measurements made as a function of photon energy allow the most careful comparisons with theoretical calculations. Largely because of relative experimental and theoretical simplicity, the most extensive studies have been done on the noble-gas atoms, but recent experiments have been carried out on other elements as well.[4]

While the first measurements of angular distributions in photodetachment from negative ions were done 20 years ago,[5] only a few such measurements have been made to date,[6–14] almost all at one or two wavelengths. Sample preparation is a more difficult problem for negative ions than for neutral atoms, and experiments with those ions which can be produced with sufficient density to allow absorption measurements involve conditions which are not very favorable for detection of detached electrons. All of the measurements of angular distributions of photodetached electrons have been done using laser-photodetached-electron spectrometry of negative-ion beams.[15] In these experiments, a mass-selected negative-ion beam crosses the focal waist of a cw (usually argon-ion) laser, and the electrons photodetached into a narrow cone perpendicular to both the ion and laser beams are collected and energy analyzed. The angular distribution of electrons is obtained by measuring the electron current as a function of the angle of the polarization of the linearly polarized laser beam. The large photon fluxes available with laser sources make possible measurements with good signal-to-noise ratios, but a limited range of photon energies is available.

This paper reports measurements of the angular distribution of electrons photodetached from negative atomic oxygen ions at five photoelectron kinetic energies ranging from 0.24 to 1.25 eV. The experiments were done using a collinear laser–ion-beam apparatus where the detached electrons were collected from a 20-cm-long section of the beam. O^- was chosen for this study because of its relative ease of production, the availability of suitable lasers for photodetachment, the fine structure is small enough that photoelectron energy analysis is not required, and because it is one of the few negative ions for which a calculation has been carried out.[16–20] In addition to presenting the experimental results, we briefly discuss the calculation of angular distributions, compare the experimental results to the calculation by Cooper and Zare,[16] and discuss the information about the transition matrix elements contained in the experimental results.

II. EXPERIMENTAL TECHNIQUE

In general, the differential cross section for production of photoelectrons from an unpolarized target by incident linearly polarized light in the electric dipole approximation is written as

$$\frac{d\sigma}{d\Omega}=\left[\frac{\sigma}{4\pi}\right][1+\beta P_2(\cos\theta)]\ , \tag{1}$$

where σ is the total cross section, β is the asymmetry parameter, $P_2(\cos\theta)=(3\cos^2\theta-1)/2$, and θ is the angle between the polarization vector of the incident light and the direction of the photoelectron. The experiment consisted of measuring the photoelectron yield with a fixed detector as the polarization of the light was rotated and extracting a value for β for a number of laser wavelengths to give β as a function of photoelectron energy.

A schematic diagram of the experimental apparatus is shown in Fig. 1. Negative oxygen ions were produced in a negative-surface-ionizer ion source[21] and accelerated to 2.5 keV. After being mass analyzed in a magnetic isotope separator, the ions entered a 1.2-m-long drift region where they were overlapped with a collinear laser beam.

 ©1989 The American Physical Society

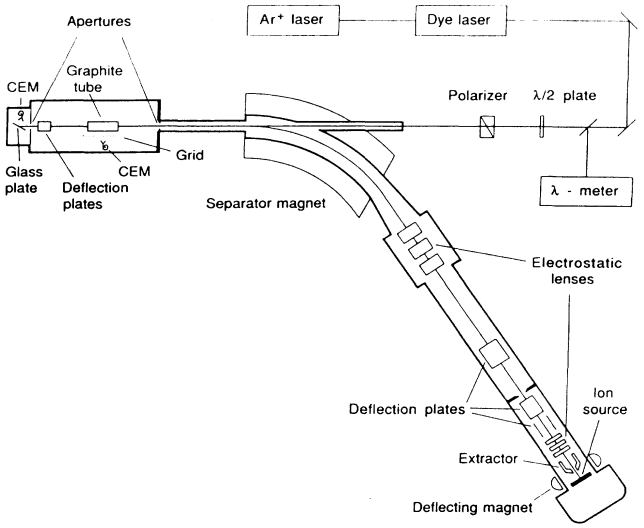

FIG. 1. Schematic diagram of the experimental apparatus.

Both the neutral atoms and the electrons produced in the photodetachment process was detected. The neutral atoms were detected after the drift region, while those electrons detached into a limited solid angle in the middle of the drift region were detected in that region.

The negative surface ionizer consists of LaB_6 (work function, 2.7 eV; melting point, 2210 °C) pressed on the surface of a tantalum rod. Before use, the 1-mm^2 spot of LaB_6 was sintered by heating to 1400 °C for a few minutes. Typical operating conditions were a LaB_6 temperature of 1200 °C and a source pressure of 1.5×10^{-5} Torr of O_2. These conditions produced a stable ion current of approximately 1 nA, which gradually decreased with time. The lifetime of the source was approximately 40 h. The oxygen ions are probably not produced in a surface-ionization process. An electron-capture process in the region just outside the ionizer is more probable.

The ions were extracted from the source through a 4-mm-wide and 10-mm-long channel. After passing through two electrostatic lenses and three pairs of deflection plates, the ions were mass analyzed in a 55° double-focusing magnet. Finally, the ions entered the drift region, defined by two apertures with a diameter of 3 mm placed 1.2 m apart. To achieve a reasonably parallel and homogeneous ion beam, the area of the ion beam was made larger than the area of the entrance aperture. This also reduced ion-beam-intensity fluctuations in the drift region due to small variations in the ion-beam parameters.

A pair of deflection plates placed in front of the second drift-region aperture were used to separate the ions from the neutral atoms produced in the drift region. The ions and neutral atoms were detected by letting them impinge on a glass plate after the second aperture and measuring the secondary electrons produced on the plate with a channel electron multiplier (CEM). The glass plate was covered with a thin conducting layer of tin-doped indium oxide (In_2O_3:Sn) to prevent charging of the plate. The bias voltage of the front cone of the CEM was adjusted so that a large but not saturated signal was obtained. The pulses from the CEM were amplified and counted. The neutral beam typically produced a count rate of 20 kHz.

Two different lasers were used. An argon-ion laser (Innova 100) was used to produce wavelengths of 514, 488, and 458 nm, and a ring dye laser (CR 699-21) was used to produce wavelengths of 589 nm (Rhodamine dye) and 727 nm (Pyridine 1). The linearly polarized light from the laser passed through a $\lambda/2$ plate and a Glan-Thomson polarizing prism (extinction ratio 10^{-5}) and finally entered the vacuum chamber perpendicular to a flat glass window. The polarization of the light could be adjusted to any desired angle by rotating the $\lambda/2$ plate and the polarizer prism. The normal incidence of the light on the vacuum-system window permitted rotation of the polarization with a minimum of intensity variation. The laser beam merged with the ion beam after it exited from the mass-selecting magnet. To minimize variations in the spatial overlap of the laser and ion beams, the laser beam was made smaller than the ion beam (which had a diameter of 3 mm). Two lenses were used in the laser beam to get a thin (diameter 0.8 mm), nearly parallel laser beam with its focus in the middle of the interaction region.

A 25-cm-long graphite tube with an inner diameter of 1.3 cm and an outer diameter of 3.2 cm was placed in the middle of the drift region. The ion beam traveled through the center of the tube (here called the interaction region). A row of 67 small holes, 2.5 mm in diameter, was drilled in one side of the tube to allow electrons to escape from the interaction region. This geometry allowed only those electrons emitted perpendicular to the beam (in the horizontal plane) and with a certain angle to the plane of polarization of the laser beam to emerge from the interaction region. A stainless-steel mesh with a transmission of 30% was placed just outside the holes in the graphite tube, and electrons which passed through the mesh were collected using a bias of 60 V on the cone of a CEM. Just as for the neutral atoms, the signal from the CEM was amplified and counted.

A great deal of care was taken in order to make the interaction region field free. Use of magnetic materials was avoided. The vacuum chamber was enclosed in three pairs of Helmholtz coils and the interaction region magnetically shielded with two layers of mu-metal. The residual magnetic field was measured with a Hall-probe gaussmeter to be less than 10^{-6} T. To avoid problems with contact potentials, only one material was used in the interaction region. Graphite was chosen because of its stability against contact potential changes. High voltages from the CEM's and the deflection plates were carefully shielded with copper plates and meshes to avoid stray fields.

The vacuum in the interaction region was typically 4×10^{-7} Torr. This was achieved with a diffusion pump with a freon-cooled baffle and a liquid-nitrogen trap. A better vacuum would have been desirable since collisionally detached electrons gave a significant background.

Another initial source of background electrons was secondary electrons produced when the ion beam impinged on the edges of the first aperture. These electrons were blocked with copper plates with slightly larger holes placed just behind the aperture.

III. MEASUREMENTS AND RESULTS

For all of the measurements the count rates of electrons and neutrals were collected simultaneously. The data were taken alternately with and without the laser beam blocked. The data with no light were necessary to determine the background of collisionally produced electrons and neutral atoms. The numbers of photodetached electrons and neutral atoms were obtained from the differences in the data with and without light. The count rate of the photodetached neutral atoms was used as normalization to reduce the effects of laser- and ion-beam-intensity variations.

In the initial stages of the experiment, the 488-nm line from the argon-ion laser was used to photodetach the electrons. The electron intensity was measured as the polarization of the light was rotated in 10° steps between $\theta=0°$ and 180°. To reduce the influence from long-term drifts, the intensity at 90° was measured before and after each measurement at another angle, and the results were normalized to the intensity at 90°. The normalized experimental data are shown in Fig. 2. As can be seen in the figure, the signal-to-noise ratio is about 40:1, and the data are symmetric about $\theta=90°$.

In order to interpret the experimental results properly, two important effects have to be considered. The first is a kinematic effect discussed by Siegel *et al.*[6] The nonnegligible velocity of the ion beam causes a difference in the center-of-mass system and in the laboratory system. Electrons which are collected perpendicular to the ion beam in the laboratory must have been ejected backwards in the center-of-mass frame with a velocity equal to that of the beam. The effect on the observed angular distribution is largest when $\theta=0°$ and decreases to zero when $\theta=90°$. Every electron emitted forward or backward is ejected perpendicular to the polarization direction when $\theta=90°$.

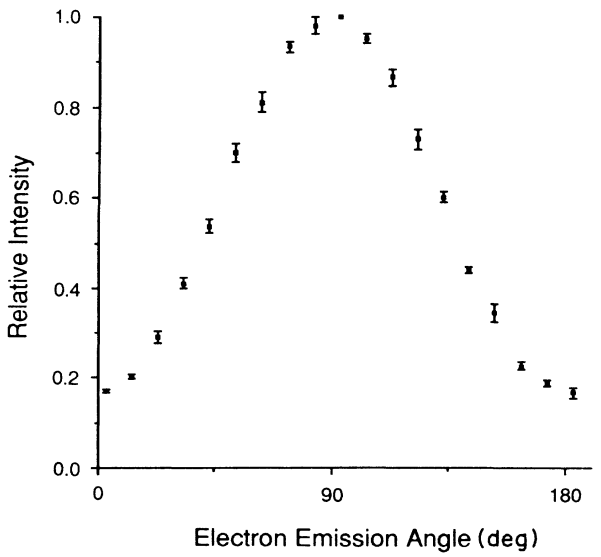

FIG. 2. Angular distribution of electrons photodetached from O^- at 488 nm. The electron count rate, normalized to that at 90°, is plotted as a function of the angle between the light polarization and the direction of the ejected electron. Corrections for a kinematic effect and for acceptance angles are made before using the data to extract a value for the asymmetry parameter β.

The second effect to be taken into account is the fairly large acceptance angle in our experiment. The geometric acceptance angle is ±6° in the vertical plane, and the angle is ±15° in the horizontal direction due to the extension of the ion beam in the horizontal plane. The effective vertical acceptance angle equals the geometrical acceptance angle, while the effective horizontal acceptance angle depends upon the polarization of the light. If $\theta=90°$ (electric vector vertical), every electron emitted in the horizontal plane is perpendicular to the electric vector. Thus the effective horizontal acceptance angle is equal to zero. If $\theta=0°$ (electric vector horizontal), the effective acceptance angle will be as large as ±15°. Both the kinematic and angular acceptance effects are larger for $\theta=0°$ and act to reduce the contrast between the $\theta=0°$ and 90° results. These effects are included when the value of β is extracted from the data. The kinematic correction is much larger than the correction for angular acceptance, but can be calculated accurately. For wavelengths other than 488 nm, only the intensities at $\theta=0°$ and 90° were used to determine β. At these angles, the effect of a possible misalignment of the polarization direction is a minimum.

The experimental results are presented in Table I along with a comparison to previous results at 488 nm by Hall and Siegel[5] and at 488 and 514 nm by Breyer, Frey, and Hotop.[10] The uncertainty given includes statistical (two standard deviations) and estimated systematic errors. The influence of magnetic fields, of depolarization of the laser light, and of polarization of the ion beam and of ions other than O^- in the ion beam has been verified to be negligible. Only errors due to misalignment of the laser and ion beams with respect to the center of the graphite tube are included as systematic errors. These are estimated to change the value of β extracted from the data by less than 1%. This error was added to the statistical error to produce the result given in Table I.

Another possible source of error in the result arises from reflection of electrons from the graphite surfaces. Reflection,[22] rather than absorption, of electrons increases the angular acceptance and hence reduces the magnitude of β derived from the data. If we assume that electrons reflected from the surface are scattered isotropically into a solid angle of 2π and that 25% of the electrons hitting the graphite are reflected, a ratio of intensities of photoelectrons at 0° and 90°, given in Table I as I_0/I_{90}, could change by 0.015. At 488 nm this corresponds to a change in β of 0.02. It is possible that this is the reason why our measured values of β are slightly

TABLE I. Results from the present experiment compared with previous measurements. The wavelengths have been corrected for the Doppler shifts in the present experiment. I_0/I_{90} is the intensity ratio for photoelectrons emitted 0° and 90° relative to the direction of the light polarization. The measured intensity ratio is corrected for a kinematic effect and non-negligible acceptance angles before extracting a value for the asymmetry parameter β. The errors quoted for β include statistical errors (two standard deviations) and an allowance for a small possible systematic error due to laser- and ion-beam alignment. The values quoted from Ref. 10 are averaged over the fine structure.

Wavelength (nm)	I_0/I_{90} measured	I_0/I_{90} corrected	β (this work)	β^a	β^b
458.2	0.207(6)	0.137(16)	−0.808(20)		
488.3	0.170(3)	0.087(13)	−0.876(18)	−0.885(15)	−0.909(19)
514.8	0.172(4)	0.078(14)	−0.888(20)		−0.919(11)
589.3	0.216(13)	0.083(23)	−0.881(32)		
727.6	0.661(57)	0.47(7)	−0.43(7)		

[a]Reference 5.
[b]Reference 10.

smaller in magnitude than the values obtained by Breyer, Frey, and Hotop at 488 and 514 nm. Stray electric fields could also change the effective acceptance angle. The use of graphite in the interaction region should minimize any stray electric fields, and the effect on electrons with energies of 0.3 eV or greater should be minimal.[23]

IV. INTERPRETATION OF THE RESULTS

In the central-potential model,[3] β for photodetachment of an electron with initial orbital angular momentum l is given by the Cooper-Zare[16] formula

$$\beta=\frac{l(l-1)R_{l-1}^2+(l+1)(l+2)R_{l+1}^2-6l(l+1)R_{l+1}R_{l-1}\cos(\delta_{l+1}-\delta_{l-1})}{(2l+1)[lR_{l-1}^2+(l+1)R_{l+1}^2]}, \tag{2}$$

where $R_{l\pm1}$ are the dipole radial matrix elements and $\delta_{l\pm1}$ are the phase shifts. For photodetachment of O^-, $l=1$ and the continuum states are s and d waves.

Cooper and Zare used the semiempirical potential of Robinson and Geltman[24] to calculate β for a few negative ions. Their results for O^- are shown as a solid line in Fig. 3 along with the data of the present experiment. Also shown in Fig. 3 are results obtained from Eq. (2) using simple assumptions about the negative ion. The dot-dash line is the result of the very simplest assumptions. If we assume that the final-state wavelength is large compared to the size of the initial state (an assumption that is reasonably well satisfied only for part of the range of photoelectron energies shown), and if we assume that there is no interaction between the continuum-state electron and the neutral atom, we obtain a simple energy dependence of the radial matrix elements, $R_{l\pm1}\propto k^{l\pm1}$, where k is the wave number of the continuum electron. (This energy dependence of the matrix elements corresponds to Wigner-law[25] behavior of the cross section, which has been shown to apply to a number of negative ions, including O^-, at least near threshold.[15,26] Here we use this energy dependence only in the ratio of the matrix elements for the two continuum channels, and it may continue to be valid at energies where the cross section for either channel shows significant deviation from Wigner-law behavior.) Also, in this limit, there is no phase shift between the two outgoing waves and $\cos(\delta_{l+1}-\delta_{l-1})=1$. Since $R_2/R_0\propto k^2$, we can set $R_2/R_0=A_2\varepsilon$, where ε is the photoelectron energy and A_2 gives the relative size of the two matrix elements. (A_2 is a measure of the size of the negative ion; in the limit of zero size $A_2=0$.) Setting $l=1$ in Eq. (2) and substituting $A_2\varepsilon$ for R_2/R_0 and c for $\cos(\delta_2-\delta_0)$ ($c=1$ in the simplest case), we obtain

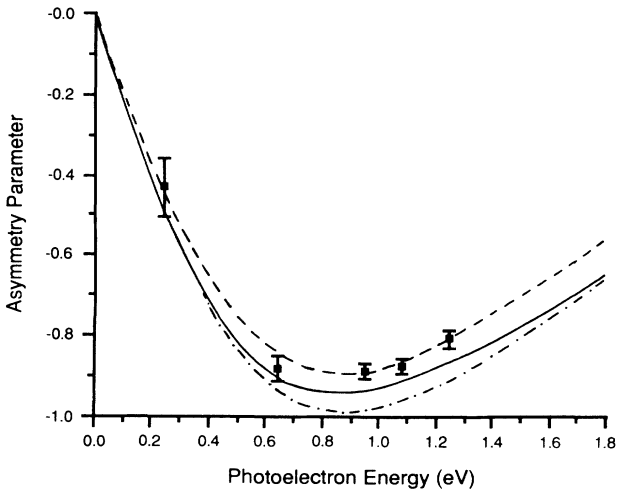

FIG. 3. Experimental results for the asymmetry parameter plotted as a function of photoelectron energy together with the results of the calculation by Cooper and Zare (Ref. 16) (solid line) and with the results of a simple expression for β discussed in the text with $\cos(\delta_2-\delta_0)=1$ (dot-dash line) and $\cos(\delta_2-\delta_0)=0.925$ (dashed line).

$$\beta = 2A_2\varepsilon(A_2\varepsilon - 2c)/(1+2A_2^2\varepsilon^2) .$$

This expression for β with $c=1$ and A_2 adjusted to give the minimum at the position of the minimum in the Cooper-Zare calculation is what is plotted as the dot-dash line in Fig. 3.

We see from Fig. 3 that this very simple model qualitatively reproduces the behavior of the asymmetry parameter as a function of energy that is predicted by the more realistic Cooper-Zare calculation. Thus the overall shape of the curve reflects largely the short-range behavior of the negative-ion potential. Very similar shapes near threshold were calculated by Radojevic, Kelly, and Johnson for asymmetry parameters in photodetachment from the halogen negative ions.[20] The simple formula says that β starts at zero at threshold (pure s wave) and falls due to interference between the s and d channels to a minimum value at a position where $R_2/R_0=0.5$ and rises again toward the limiting value of $\beta=+1$ characteristic of pure d wave. The minimum is characteristic of negative ions. For photoionization of p shells of neutrals, the Coulomb phase shift between the s and d waves gives $c=-1$ at threshold, and β is positive near threshold.[2]

The experimental data lie slightly above the Cooper-Zare curve in Fig. 3. Examination of the expression for β shows that the position of the minimum depends largely on the value of A_2, while the depth of the minimum is dependent mainly on c, i.e., the size of the phase shift. If we adjust c to give a depth equal to that of the Cooper-Zare curve, we find $c=\cos(\delta_2-\delta_0)=0.96$, consistent with the value of 0.955(10) obtained directly from the calculation and quoted by Breyer, Frey, and Hotop.[10] The dashed line also plotted in Fig. 3, which falls very close to the data, is obtained using $A_2=1.1$ eV^{-1} and $c=0.925$. Uncertainties in the magnitudes of β near the minimum, arising from such things as electron reflection, directly affect the corresponding value of the phase shift, and thus our results should not be taken to be inconsistent with the Cooper-Zare value. Systematic changes in the value of β have a smaller effect on the position of the minimum and thus on the corresponding value for the ratio of the sizes of the s and d wave cross sections.

V. CONCLUSIONS

Measurements of the asymmetry parameter β have been made for photodetachment of O^- in the vicinity of the first minimum of β. This minimum is characteristic of photodetachment from a p orbital in a short-range potential. Values for the phase shift and the ratio of the sizes of the s and d wave cross sections are obtained by comparison of the data with a simple expression for β.

ACKNOWLEDGMENTS

We wish to thank the nuclear physics group at Chalmers University of Technology for giving us permission to use their ion accelerator. We are indebted to S. Wilhelmsson for teaching us how to run this apparatus and K. Peterholm for technical assistance during the reconstruction. Professor I. Lindgren and Dr. T. Olsson are acknowledged for support and discussions. This work was supported by the Swedish Natural Science Research Council (NFR). One of us (D.J.L.) would like to acknowledge the hospitality of Professor I. Lindgren and the Department of Physics at Chalmers University of Technology during the initial stages of this work and the partial support of the U.S. National Science Foundation.

[1]A number of reviews of photoionization experiments, including measurements of angular distributions have been published. See, for example, J. A. R. Samson, in *Corpuscles and Radiation in Matter I*, Vol. 31 of *Handbuch der Physik*, edited by W. Mehlhorn (Springer-Verlag, Berlin, 1982), pp. 123–213; B. Sonntag and F. Wuilleumier, Nucl. Instrum. Methods **208**, 735 (1983); M. O. Krause, Aust. J. Phys. **39**, 601 (1986).

[2]A. F. Starace, in *Corpuscles and Radiation in Matter I*, Ref. 1, pp. 1–121; H. P. Kelly, in *Atomic Physics 8*, edited by I. Lindgren, A. Rosen, and S. Svanberg (Plenum, New York, 1983), pp. 305–337.

[3]S. T. Manson and A. F. Starace, Rev. Mod. Phys. **54**, 389 (1982).

[4]See, for example, R. Malutzki, M. S. Banna, W. Braun, and V. Schmidt, J. Phys. B **18**, 1735 (1985); B. H. McQuaide, M. S. Banna, P. Gerard, and M. O. Krause, Phys. Rev. A **35**, 1603 (1987).

[5]J. L. Hall and M. W. Siegel, J. Chem. Phys. **48**, 943 (1968).

[6]M. W. Siegel, R. J. Celotta, J. L. Hall, J. Levine, and R. A. Bennett, Phys. Rev. A **6**, 607 (1972); R. J. Celotta, R. A. Bennett, J. L. Hall, M. W. Siegel, and J. Levine, *ibid.* **6**, 631 (1972).

[7]H. Hotop, R. A. Bennett, and W. C. Lineberger, J. Chem. Phys. **58**, 2373 (1973).

[8]R. J. Celotta, R. A. Bennett, and J. L. Hall, J. Chem. Phys. **60**, 1740 (1974).

[9]A. Kasdan and W. C. Lineberger, Phys. Rev. A **10**, 1658 (1974).

[10]F. Breyer, P. Frey, and H. Hotop, Z. Phys. A **286**, 133 (1978).

[11]F. Breyer, P. Frey, and H. Hotop, Z. Phys. A **300**, 7 (1981).

[12]P. C. Engelking and W. C. Lineberger, J. Chem. Phys. **66**, 5054 (1977).

[13]P. C. Engelking, R. R. Corderman, J. J. Wendoloski, G. B. Ellison, S. V. O'Neil, and W. C. Lineberger, J. Chem. Phys. **74**, 5460 (1981).

[14]P. Frey, M. Lawen, F. Breyer, and H. Klar, Z. Phys. A **304**, 155 (1982).

[15]A brief discussion of experimental techniques, without explicit mention of angular distribution measurements, is given by H. Hotop and W. C. Lineberger, J. Phys. Chem. Ref. Data **14**, 731 (1985).

[16]J. Cooper and R. N. Zare, J. Chem. Phys. **48**, 942 (1968).

[17]R. M. Stehman and S. B. Woo, Phys. Rev. A **20**, 281 (1979); **23**, 2866 (1981).

[18]C. M. Lee, Phys. Rev. A **11**, 1692 (1975).

[19]U. Fano and C. H. Greene, Phys. Rev. A **22**, 1760 (1980).

[20]V. Radojevic, H. P. Kelly, and W. R. Johnson, Phys. Rev. A **35**, 2117 (1987).

[21]H. Kawano and F. M. Page, Int. J. Mass Spectrom. Ion Phys. **50**, 1 (1983); M. Martenson and S. Wilhemsson, Nucl. In-

strum. Methods B **12**, 273 (1985); Int. J. Mass Spectrom. Ion Process. **67**, 179 (1985).
[22]H. Froitzheim, H. Ibach, and S. Lehwald, Rev. Sci. Instrum. **46**, 1325 (1975); N. L. S. Martin and A. von Engel, J. Phys. D **10**, 863 (1977).
[23]H. Ibach and D. L. Mills, *Electron Energy Loss Spectroscopy and Surface Vibrations* (Academic, New York, 1982), Sec. 2.8.2
[24]E. J. Robinson and S. Geltman, Phys. Rev. **153**, 4 (1967).
[25]E. P. Wigner, Phys. Rev. **73**, 1002 (1948).
[26]D. M. Neumark, K. R. Lykke, T. Andersen, and W. C. Lineberger, Phys. Rev. A **32**, 1890 (1985).